Stanford Exploration Project, Report 114, October 14, 2003, pages 99–108

Velocity estimation for seismic data exhibiting focusing-effect AVO (Part 3)

Ioan Vlad, Biondo Biondi, and Paul Sava[1]

ABSTRACT

Given a satisfactory image perturbation, Target Image Fitting (TIF) Wave Equation Migration Velocity Analysis (WEMVA) successfully produces a velocity model that completely eliminates focusing-effect AVO anomalies through prestack depth migration. However, TIF WEMVA ceases to converge to the desired result when the Born approximation is not fulfilled because the starting guess is too far from the correct velocity. Fortunately, there are several possible remedies to this problem. Extracting the image perturbation proves somewhat more complicated than expected, but new possible solutions based on differential semblance have been identified.

INTRODUCTION

Focusing-effect AVO (FEAVO) consists of focusing seismic wavefield amplitudes through velocity lenses too small to generate proper triplications. The amplitude effects are large enough to thwart proper AVO analysis in the affected area (Kjartansson, 1979). Migration with a velocity model containing the lenses that cause FEAVO eliminates the effect (Bevc, 1994). However, the traveltime effects are too small to allow classical velocity analysis approaches such as Dix inversion or traveltime tomography to succeed. New approaches are needed to deal with such small velocity anomalies.

In previous work (Vlad and Biondi, 2002; Vlad, 2002) Wave-Equation Migration Velocity Analysis (WEMVA; introduced by Biondi and Sava (1999)) was shown to resolve FEAVO-causing velocity anomalies, by optimizing image quality in the angle domain after prestack depth migration. The first step of the proof consisted in showing that FEAVO anomalies are recognizable in a field dataset migrated and transformed to the angle domain. WEMVA iterates by migrating with the current velocity model, extracting an image perturbation, and converting it into a velocity model update by inverting a linearized downward continuation operator. Vlad (2002) then showed that the inversion operator did not distort FEAVO anomalies into becoming unrecognizable, despite the linearizing approximations.

While the previous studies only demonstrated the possible suitability of WEMVA as a tool for the given problem, this paper shows the results of successfully running WEMVA on a FEAVO-affected synthetic dataset. In particular, it shows that the velocity lenses are

[1]**email:** nick@sep.stanford.edu, biondo@sep.stanford.edu, paul@sep.stanford.edu

found, and that the image migrated with the updated velocity model no longer exhibits FEAVO effects. This paper also explores the limitations of the type of WEMVA used and different ways of extracting the image perturbation to be fed into the inversion.

FEAVO BEFORE MIGRATION

We have generated two 2-D synthetic datasets, using two velocity models. The purpose of the first one is to show that FEAVO anomalies are indeed eliminated when migrating with a velocity model obtaine by WEMVA. The purpose of the second one is to test what happens when the velocity anomalies are outside the range within which TIF WEMVA is accurate. We will denote the two datasets by the names "WEMVA works" and "WEMVA breaks".

The velocity models are depicted in the same color scale in the upper panels of Figures 1 ("WEMVA works") and 2 ("WEMVA breaks"). The background velocity is 2000 m/s for both. The peak anomalies, from left to right, as departures from the background, are (in m/s): -153, -188, +231 for the "WEMVA works" velocity model and -586, -766, +519 for the "WEMVA breaks" velocity model.

The "WEMVA works" velocity anomalies cause visible amplitude focusing, but minimal traveltime anomalies (middle panel in Figure 1). The intense "WEMVA breaks" velocity lenses, on the other hand, cause visible triplications and departures from hyperbolicity (middle panel in Figure 2). The specific signature of FEAVO before migration can be examined in both cases by squaring each of the values in the data cube, then summing along the time axis. The results of this operation is shown in the lower panels of Figures 1 and 2 respectively. The axes of the image are midpoint and offset, and specific "V" shapes are visible for each of the three velocity anomalies.

It is interesting to compare these FEAVO effects with those present in the only field dataset currently available to us that exhibits FEAVO anomalies. The dataset in question is the Grand Isle dataset analyzed by Kjartansson (1979) – the original dataset on which FEAVO was defined. The FEAVO effects in it are comparable with those in the lower panels of Figures 1 and 2 because the background velocities are approximately similar. Given that the intensity of the effects is linked to the magnitude of the velocity anomalies, we can empirically estimate that the deviation of the Grand Isle velocity anomalies from the background is around 200-300 m/s. Since the "thickness" of the V's is linked to the dimensions of the velocity lenses, we can also infer that they are approximately 20-30m in diameter.

WEMVA ELIMINATES SYNTHETIC FEAVO

As described by Sava and Symes (2002), the image perturbation to be fed into WEMVA can be created by Target Image Fitting (TIF), or by Differential Semblance Optimization (DSO, Symes and Carazzone (1991), Chauris and Noble (1998)). We chose the TIF approach because the purpose of this test was to determine conclusively whether WEMVA-produced velocity models can eliminate realistic FEAVO effects independent of image perturbation extraction.

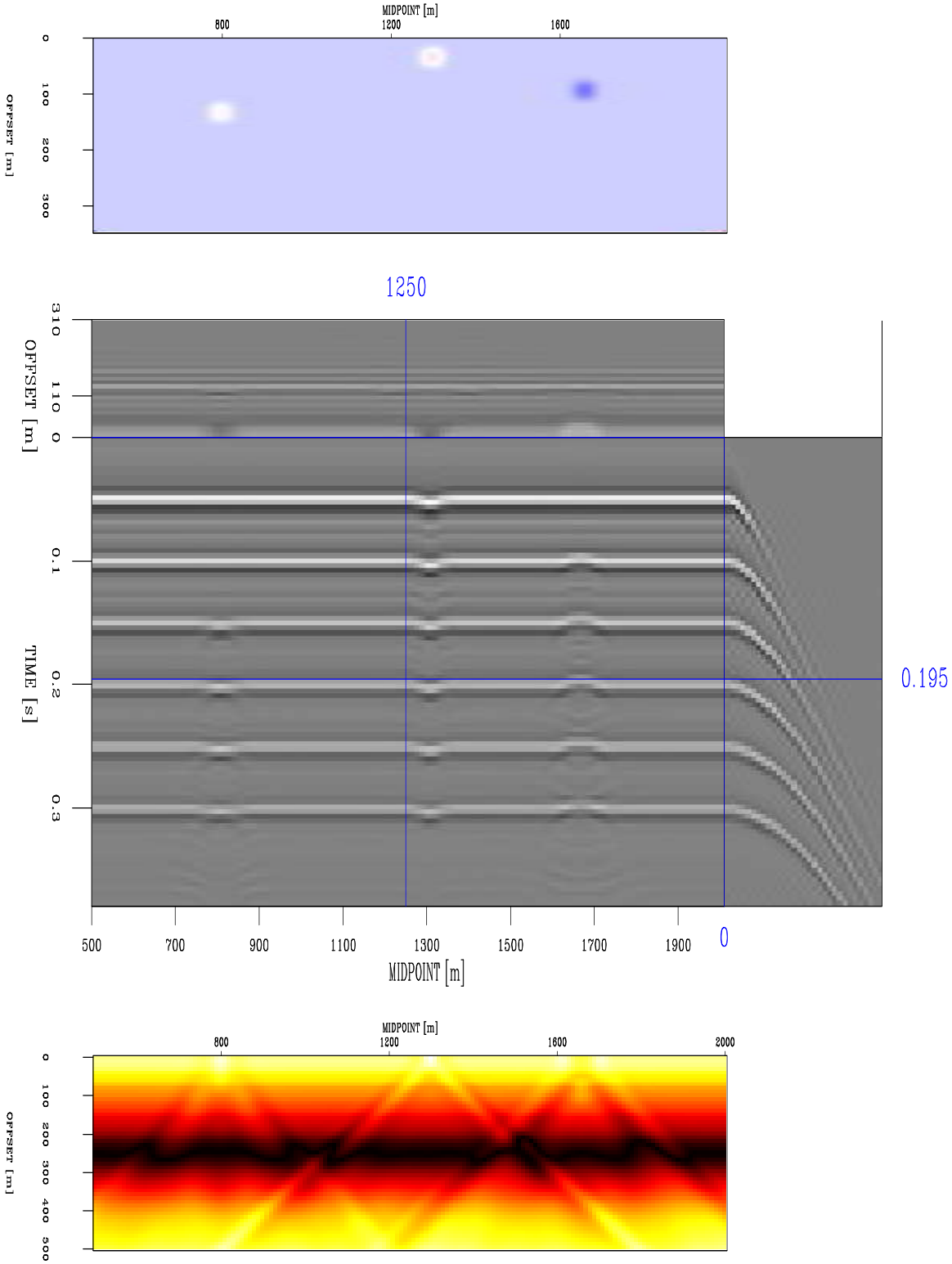

Figure 1: "WEMVA works" case: velocity model, dataset and FEAVO effects. The velocity model has the same color scale as the one in the upper panel of Figure 2. nick1-f1 [CR]

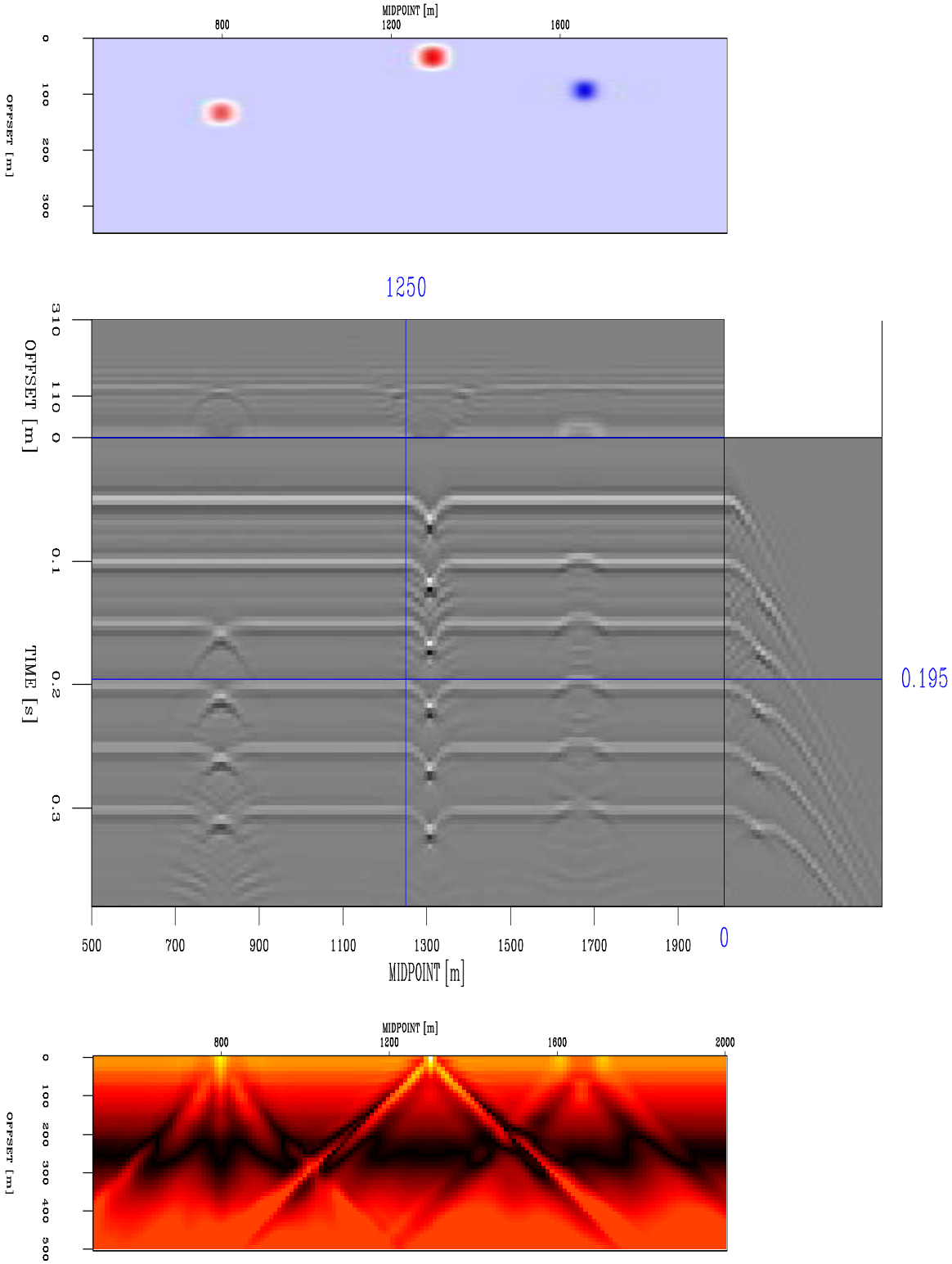

Figure 2: "WEMVA breaks" case: velocity model, dataset and FEAVO effects nick1-f2 [CR]

Since the dataset is synthetic and the correct velocity model known, we were able to generate an optimal image perturbation by subtracting the image migrated with the current velocity from the one migrated with the correct velocity.

We used the "WEMVA works" dataset. The starting estimate for the first WEMVA iteration was the 2000 m/s background velocity. FEAVO effects in a slice from the angle-domain image migrated with the background velocity are shown in the upper panel of Figure 4.

We ran 10 conjugate-gradient solver iterations, then updated the velocity model. The resulting model is shown in the upper panel of Figure 3. Its peak anomalies as departures from the background, in m/s, from left to right, are: -74, -84, +99. We migrated with this velocity model. FEAVO effects in a slice from this image are shown in the middle panel of Figure 4. They are weaker now, but still visible.

We performed another WEMVA inversion loop, with 10 solver iterations, starting from the updated velocity model. The resulting velocity model is shown in the bottom panel of Figure 3. Its peak anomalies as departures from the background, in m/s, from left to right, are: -105, -123, +149. The angle-domain image obtained by migrating with this new velocity model are shown in the lower panel of Figure 4. The FEAVO effects are no longer recognizable. When WEMVA's assumptions, discussed in the next section, are satisfied and the image perturbation can be extracted in a satisfactory manner, the inversion process converges and the resulting velocity field is accurate enough to reliably eliminate FEAVO effects.

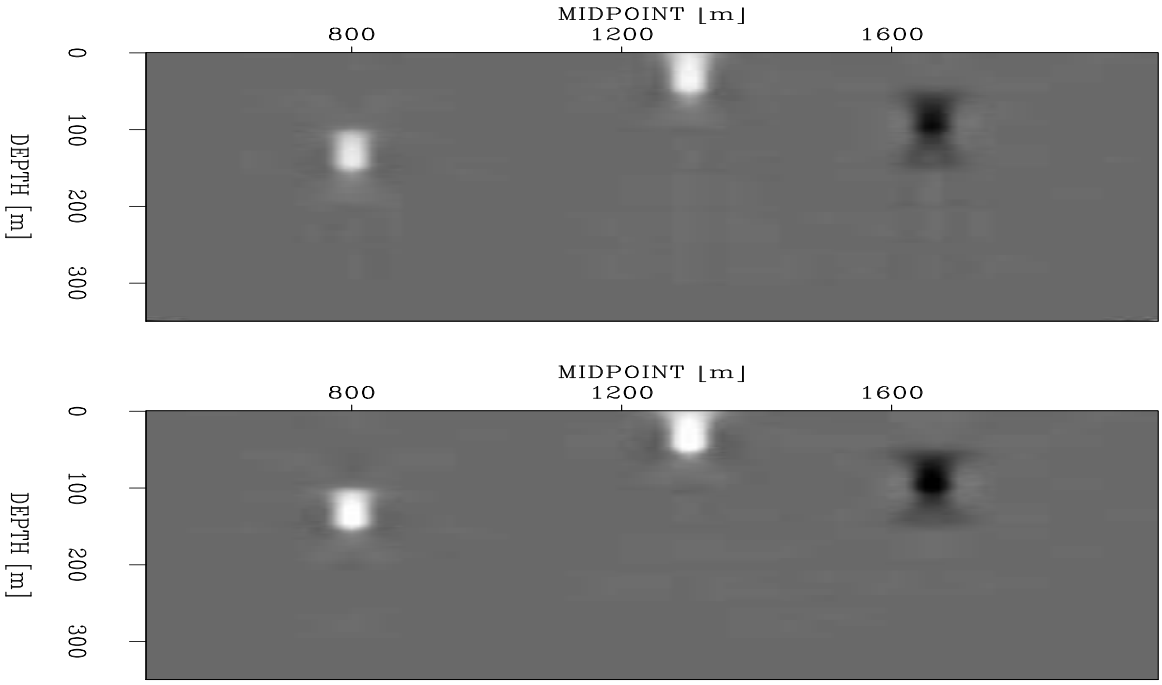

Figure 3: **Upper panel:** velocity model updated after one WEMVA iteration. **Lower panel:** velocity model updated after a second WEMVA iteration. Both panels are represented in the same color scale. nick1-f3 [CR]

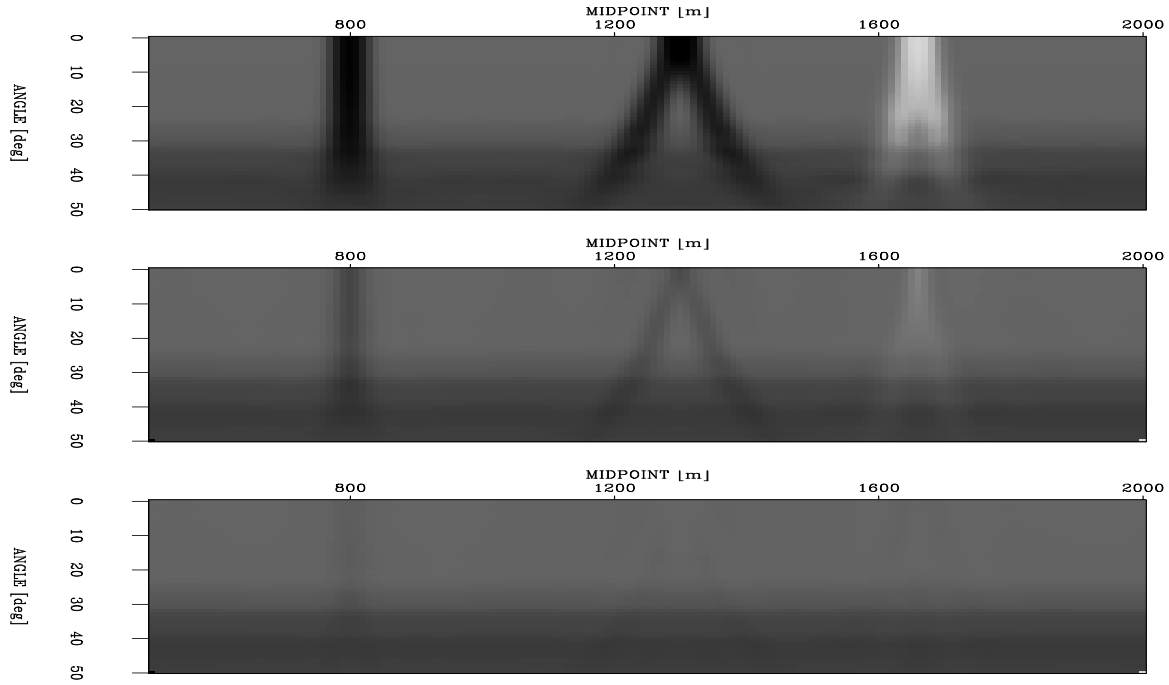

Figure 4: Angle-domain slices at a depth of 155m. **Upper panel:** from the image obtained with the constant background velocity; **Middle panel:** from the image obtained with the velocity in the upper panel of Figure 3; **Lower panel:** from the image obtained with the velocity in the lower panel of Figure 3. nick1-f4 [CR]

WEMVA LIMITATIONS

The most important limitation of WEMVA is the range of validity of its assumptions. In the case of the Born approximation in TIF WEMVA, phase differences caused by the true velocity anomalies in the image must be smaller than $\pi/4$. The corresponding velocity anomaly magnitudes vary with the range of frequencies present in the dataset and with the spatial extent of the anomalies.

We performed one WEMVA pass with 10 conjugate-gradient solver iterations on the "WEMVA breaks" dataset. In this instance the phase differences caused by the velocity anomalies are too large to be satisfactorily approximated in a Born manner. The velocity update thus obtained is presented in Figure 5. It does not converge toward the true anomalies like the corresponding update in the upper panel of Figure 3. Since this occurs when using the ideal image perturbation, inaccuracies in extracting the perturbation would only amplify the trend.

There are several possible avenues for avoiding either the Born approximation limitations or the Born approximation altogether: 1. obtaining a very good velocity starting guess with other velocity analysis methods; 2. creating the image perturbation in connection with residual migration (Sava and Biondi, 2001); 3. employing linearizations other than Born (Sava and Fomel, 2002); 4. inverting for the lower frequencies first (Pratt, 1999); 5. using DSO WEMVA

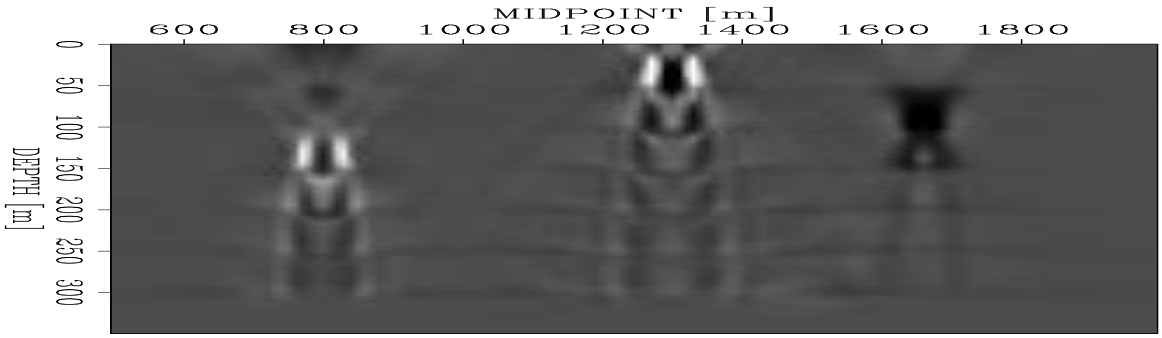

Figure 5: Velocity model updated after one WEMVA iteration comprising 10 solver iterations on the "WEMVA breaks" dataset. nick1-f5 [CR]

(Sava and Symes, 2002) where the image perturbation is extracted directly from the image using a specific operator during the inversion, without the need to find a corrected image.

EXTRACTING IMAGE PERTURBATIONS

The upper panel of Figure 6 shows the optimal image perturbation, found by subtracting the image obtained by prestack depth migration with the constant (2000 m/s) background velocity from that obtained with the correct velocity. While the absolute values of the amplitudes in the FEAVO anomalies are stronger than the background as expected, the polarities change every time the seismic wavelet alternates sign. Vlad (2002) proposed an extraction approach that would involve sweeping the image space with summations along the analytically computable shapes of the FEAVO effects. To do that, we would have to use absolute or squared values to prevent the polarity alternation from cancelling the summed values. However, discarding the information stored in the sign of the anomaly forfeits the ability to distinguish between positive and negative velocity anomalies.

There are several ways of circumventing this problem. They can be simple and cheap, but case-specific (a priori knowledge whether the lenses are faster or slower than the background). They can be more general, but also more complex and expensive (do WEMVA iterations assuming a single sign until all anomalies of that sign are eliminated, allowing anomalies of the other sign to increase; then when only increases in the image perturbations are noticed, switch the sign and start again). Even with the polarity problem, more consideration will be given in the future to the focus-filter-spread approach as envisaged by Vlad (2002) because of its potential power of eliminating the non-FEAVO noise and of exploiting the entirety of the FEAVO morphological characteristics.

The polarity conundrum mentioned above can be eliminated by identifying anomalies by their local, rather than global, characteristics. The middle panel of Figure 6 shows the image perturbation for the TIF WEMVA obtained by eliminating the DC component and by performing several other small adjustements (correcting with a cosine of the angle factor for amplitude decay, windowing away irrelevant energy at higher angles, etc). The lower panel in Figure 6

presents the velocity update obtained after one WEMVA iteration. Additional iterations did not change the result too much. The results may have improved had we used a weighting operator to mask the unresolved anomalies at higher angles (so they would not be fitted when inverting).

CONCLUSIONS

Given a satisfactory image perturbation, TIF WEMVA successfully produces a velocity model that completely eliminates FEAVO anomalies through prestack depth migration. However, TIF WEMVA ceases to converge to the desired result when the Born approximation is not fulfilled because of a velocity starting model that is too far from the correct model. Fortunately, there are several possible fixes to this problem. Extracting the image perturbation proves somewhat more complicated than expected, but we have identified and are studying possible new solutions to the problem.

REFERENCES

Bevc, D., 1994, Near-surface velocity estimation and layer replacement: SEP–**80**, 361–372.

Biondi, B., and Sava, P., 1999, Wave-equation migration velocity analysis: SEP–**100**, 11–34.

Chauris, H., and Noble, M. S., 1998, Testing the behavior of differential semblance for velocity estimation:, *in* 68th Ann. Internat. Mtg Soc. of Expl. Geophys., 1305–1308.

Kjartansson, E., 1979, Analysis of variations in amplitudes and traveltimes with offset and midpoint: SEP–**20**, 1–24.

Pratt, R. G., 1999, Seismic waveform inversion in the frequency domain, part 1: Theory and verification in a physical scale model: Geophysics, **64**, no. 3, 888–901.

Sava, P., and Biondi, B., 2001, Born-compliant image perturbation for wave-equation migration velocity analysis: SEP–**110**, 91–102.

Sava, P., and Fomel, S., 2002, Wave-equation migration velocity analysis beyond the Born approximation: SEP–**111**, 81–99.

Sava, P., and Symes, W. W., 2002, A generalization of wave-equation migration velocity analysis: SEP–**112**, 27–36.

Symes, W. W., and Carazzone, J. J., 1991, Velocity inversion by differential semblance optimization: Geophysics, **56**, no. 5, 654–663.

Vlad, I., and Biondi, B., 2002, Velocity estimation for seismic data exhibiting focusing-effect AVO: SEP–**111**, 107–123.

Vlad, I., 2002, Velocity estimation for seismic data exhibiting focusing-effect AVO (part 2): SEP–**112**, 47–64.

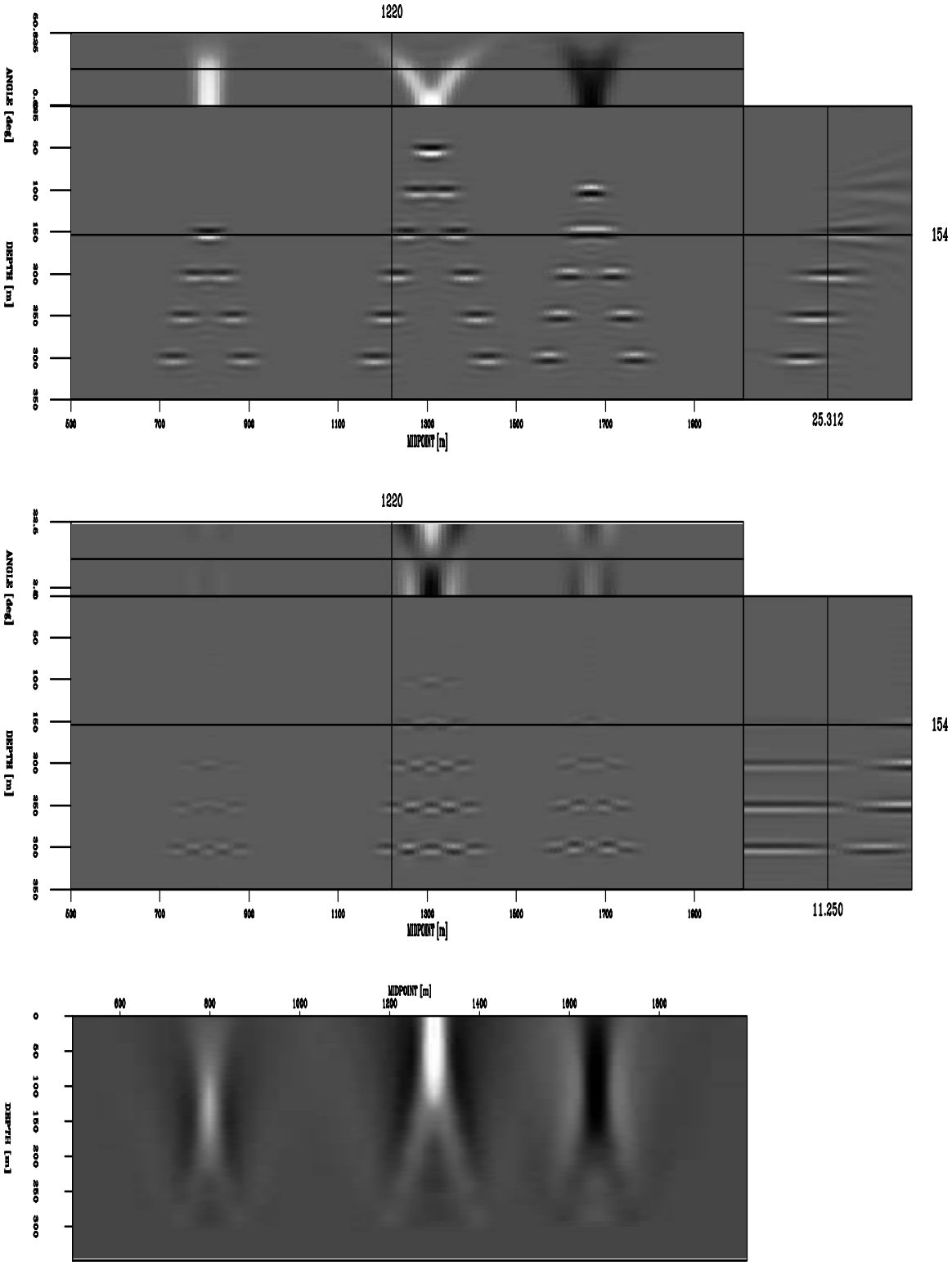

Figure 6: **Top:** ideal image perturbation for TIF WEMVA obtained by subtracting the image produced with the correct velocity and the image produced with the background velocity; **Middle:** image perturbation for TIF WEMVA obtained by processing the background velocity image in a DSO manner; **Bottom:** Velocity model obtained after one WEMVA iteration taking as input the image perturbation shown in the middle panel nick1-f6 [CR]